

| TABLE 5.1. (CONT.) | | | | | | | |
|--|--------------|-------------|----------------|-------------|----------|-------------|-----------------|
| Station Name, Start Year; Latitude, Longitude | | SON 2015 | DJF 2015/16 | MAM 2016 | JJA 2016 | SON 2016 | Jan–Dec 2016 |
| Ivittuut/ Narsarsuaq 1873; 61.2°N, 45.4°W | Anomaly (°C) | -1.8 | 0.5 | 2.8 | 1.7 | -0.1 | 1.5 |
| | z-score | -1.2 | 0.3 | 1.3 | 2.1 | 0.1 | 1.3 |
| | Max Year | 2010 | 2010 | 2010 | 2016 | 2010 | 2010 |
| | Min Year | 1874 | 1984 | 1989 | 1873 | 1874 | 1884 |
| Qaqortoq 1807; 60.7°N, 46.1°W | Anomaly (°C) | -1.3 | 1.0 | 1.8 | 1.3 | 0.2 | 1.2 |
| | z-score | -0.5 | 0.6 | 0.9 | 1.4 | 0.6 | 1.2 |
| | Max Year | 2010 | 2010 | 1932 | 1929 | 2010 | 2010 |
| | Min Year | 1874 | 1863 | 1811 | 1811 | 1874 | 1884 |
| Danmarkshavn 1949; 76.8°N, 18.7°W | Anomaly (°C) | 2.3 | 1.8 | 1.1 | 2.3 | 5.3 | 2.7 |
| | z-score | 1.7 | 1.0 | 1.0 | 3.0 | 3.3 | 3.0 |
| | Max Year | 2002 | 2005 | 1976 | 2016 | 2016 | 2016 |
| | Min Year | 1971 | 1967 | 1966 | 1955 | 1971 | 1983 |
| Illoqqortoormiut 1949; 70.5°N, 22.0°W | Anomaly (°C) | 1.1 | 2.0 | 2.6 | 2.2 | 4.2 | 2.9 |
| | z-score | 1.0 | 1.1 | 1.7 | 2.1 | 2.7 | 2.2 |
| | Max Year | 2002 | 2014 | 1996 | 2016 | 2016 | 2016 |
| | Min Year | 1951 | 1966 | 1956 | 1955 | 1951 | 1951 |
| Tasiilaq 1895; 65.6°N, 37.6°W | Anomaly (°C) | 0.5 | 2.6 | 2.9 | 2.3 | 2.3 | 2.6 |
| | z-score | 0.7 | 1.6 | 1.8 | 2.9 | 2.2 | 2.7 |
| | Max Year | 1941 | 1929 | 1929 | 2016 | 1941 | 2016 |
| | Min Year | 1917 | 1918 | 1899 | 1983 | 1917 | 1899 |
| Prins Christian Sund 1958; 60.1°N, 42.2°W | Anomaly (°C) | -0.1 | 0.4 | 1.2 | 0.8 | 1.3 | 0.9 |
| | z-score | 0.0 | 0.3 | 1.3 | 1.1 | 1.5 | 1.3 |
| | Max Year | 2010 | 2010 | 2005 | 2010 | 2010 | 2010 |
| | Min Year | 1982 | 1993 | 1989 | 1970 | 1982 | 1983 |
| Summit 1991; 72.6°N, 38.5°W | Anomaly (°C) | 0.3 | -1.3 | 4.3 | 1.2 | 2.2 | 2.2 |
| | z-score | 0.2 | -0.4 | 2.2 | 0.6 | 1.1 | 1.6 |
| | Max Year | 2002 | 2010 | 2016 | 2012 | 2002 | 2010 |
| | Min Year | 2009 | 1993 | 1992 | 1992 | 2009 | 1992 |

GBI values have been associated with extensive Greenland surface melt and negative surface mass balance (Hanna et al. 2013; McLeod and Mote 2015). Despite the near-record GBI, the average daily melt during summer of 2016 was much less than the record breaking year of 2012. A major difference between the atmospheric conditions in 2012 and 2016 was the lack of water vapor transport and associated latent heat and downwelling longwave radiative fluxes in 2016, which have recently been shown to have a considerable effect on ice sheet melt (Mattingly et al. 2016).

f. *Glaciers and ice caps outside Greenland*—G. Wolken, M. Sharp, L. M. Andreassen, D. Burgess, L. Copland, J. Kohler, S. O’Neel, M. Peltó, L. Thomson, and B. Wouters

Mountain glaciers and ice caps cover an area of over 400 000 km² in the Arctic, and are a leading contributor to global sea level change despite their relatively small volume compared to ice sheets in Antarctica and Greenland (Gardner et al. 2011, 2013; Jacob et al. 2012). Glaciers gain mass by snow accumulation and lose mass by surface melt and runoff, iceberg calving, and submarine melting where they terminate in water (ocean or lake). The total mass bal-

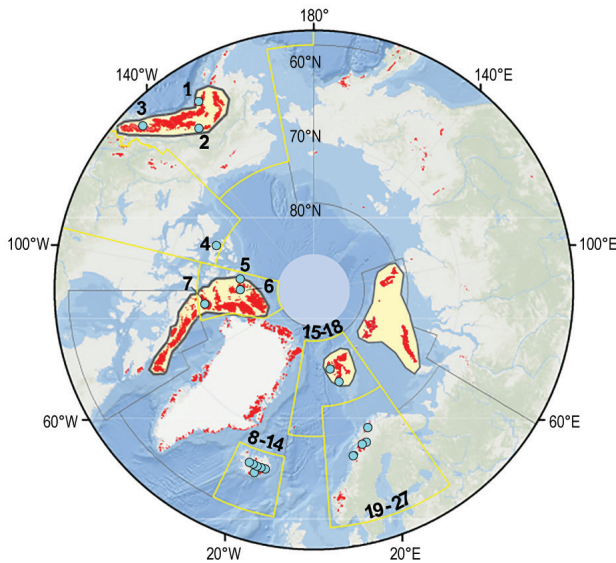


FIG. 5.14. Locations of 27 Arctic glaciers (blue circles) with long-term records of annual B_{clim} . See Table 5.2 for glacier names. Regions outlined in yellow are the Randolph Glacier Inventory (RGI) regions of the Arctic (Pfeffer et al. 2014). Individual glaciers located too close together to be identifiable on the map have numbers shown at the edge of the RGI region in which they occur. Red shading indicates glaciers and ice caps, including ice caps in Greenland outside the ice sheet. Yellow shading shows the solution domains for regional mass balance estimates for Alaska, Arctic Canada, Russian Arctic, and Svalbard derived using gravity data from the GRACE satellites (see Fig. 5.16).

ance (ΔM) is defined as the difference between annual snow accumulation and annual mass losses. Of the 27 glaciers currently monitored, only three (Kongsvegen, Hansbreen, and Devon Ice Cap NW) lose any mass by iceberg calving or melting directly into the ocean. For all glaciers discussed here, climatic mass balance (B_{clim} ; the difference between annual snow accumulation and annual runoff), a widely-used index of how glaciers respond to changes in climate, is reported.

B_{clim} values for mass balance year 2015/16 are available for only 9 of the 27 glaciers that are monitored across the Arctic (three in Alaska, one in Arctic Canada, two in Svalbard, and three in Norway), and some of these estimates are still provisional. Therefore, the focus is on the 2014/15 B_{clim} values, which are available for 23 glaciers (WGMS 2017). These glaciers are located in Alaska (three), Arctic Canada (four), Iceland (nine), Svalbard (four), and Norway (three) (Fig. 5.14; Table 5.2). For these glaciers, as a group, the average B_{clim} in 2014/15 was negative. However, all nine glaciers in Iceland and one in Norway (Engabreen) had positive balances.

For the Arctic as a whole, 2014/15 continues the negative trend of cumulative regional climatic mass

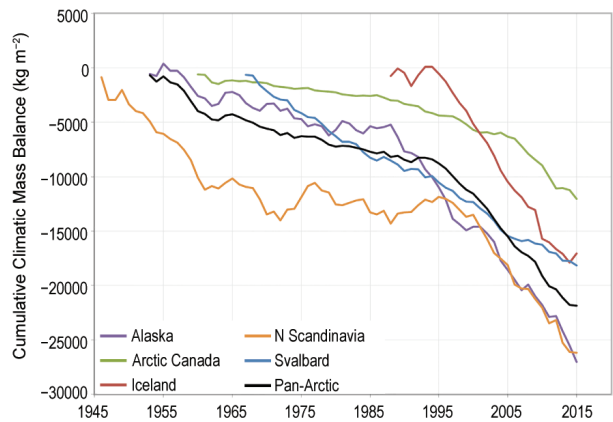


FIG. 5.15. Cumulative B_{clim} (kg m^{-2}) for glaciers in five regions of the Arctic, and for the Arctic as a whole (Pan-Arctic). Average balances are calculated for glaciers monitored in each region by summing annual averages for the period of record. Note that monitoring periods vary between regions and that the number and identity of glaciers monitored in a given region may vary between years.

balances, calculated by summing the annual average mass balances for all glaciers in each reporting region of the Arctic (Fig. 5.15). For Alaska and Arctic Canada, 2014/15 was the third most negative mass balance year on record. Climatic balances of Lemon Creek and Gulkana glaciers in Alaska were the most negative and seventh most negative, respectively, since 1966, and, for the four glaciers in Arctic Canada, they were the fourth (Meighen and Melville South ice caps) and sixth (Devon Ice Cap NW and White Glacier) most negative since 1960. The negative balances of glaciers in Alaska, Arctic Canada, and Svalbard in 2014/15 were most likely linked to melt increases caused by positive air temperature anomalies at the 850-hPa level in July–August (data from NCEP/NCAR Reanalysis; see also Fig. 5.2c). In contrast to the negative anomalies described above, 2014/15 was the second most positive mass balance year on record for Iceland, which was linked to a broad region of negative (cool) 850-hPa air temperature anomalies over the North Atlantic in June–August. These negative 850-hPa air temperature anomalies likely also resulted in melt reduction over northern Scandinavia and the least negative climatic balance for this region since 1946.

Among the nine glaciers for which 2015/16 B_{clim} measurements have been reported, the balances of glaciers in Alaska, Arctic Canada (Devon Ice Cap NW), Svalbard (Midre Lovenbreen and Austre Broggerbreen), and Norway (Engabreen, Langfjordjøkelen, and Rundvassbreen) were all negative. The pattern of negative balances continued into 2015/16 in Arctic Canada and is captured in the time series

TABLE 5.2. Measured B_{clim} of glaciers in Alaska, the Canadian Arctic, Iceland, Svalbard, and northern Scandinavia for 2014/15 and 2015/16, along with the 1981–2010 average and std. dev. for each glacier (* indicates one or more years of missing data in the climate record). Mass balance data are from the World Glacier Monitoring Service (WGMS 2017), with updates to data provided by S. O’Neel (Alaska), L. Thompson (White Glacier; Thompson et al. 2016), J. Kohler (Svalbard), and the Norwegian Water Resources and Energy Directorate (Norway; Kjølmoen et al. 2016; Andreassen et al. 2016). Numbers in left most column identify glacier locations in Fig. 5.14. Note that 2015/16 results may be based on data collected before the end of the 2016 melt season and may be subject to revision. Units for all B_{clim} are $\text{kg m}^{-2} \text{yr}^{-1}$.

| Region | Glacier (record length, years) | B_{clim} Average 1981–2010 | B_{clim} Std. dev. 1981–2010 | B_{clim} 2014/15 | B_{clim} 2015/16 |
|-----------------------------|-----------------------------------|--|--|---------------------------|---------------------------|
| Alaska | | | | | |
| 1 | Wolverine (51) | –362 | 1157 | –1100 | –500 |
| 3 | Lemon Creek (64) | –594 | 719 | –2270 | –1200 |
| 2 | Gulkana (51) | –655 | 743 | –1400 | –1300 |
| Arctic Canada | | | | | |
| 7 | Devon Ice Cap (NW) (56) | –157 | 178 | –395 | –301 |
| 5 | Meighen Ice Cap (54) | –176 | 288 | –892 | — |
| 4 | Melville South Ice Cap (53) | –303 | 373 | –1148 | — |
| 6 | White (53) | –267 | 270 | –693 | — |
| Iceland | | | | | |
| 8 | Langjökull S. Dome (19) | –1448* | 817* | 413 | — |
| 9 | Hofsjökull E (25) | –602* | 1009* | 850 | — |
| 9 | Hofsjökull N (26) | –606* | 787* | 430 | — |
| 9 | Hofsjökull SW (25) | –978* | 947* | 1380 | — |
| 14 | Köldukvislarjökull (23) | –529* | 738* | 1074 | — |
| 10 | Tungnaarjökull (24) | –1170* | 873* | 196 | — |
| 13 | Dyngjujökull (18) | –133* | 912* | 1469 | — |
| 12 | Brúarjökull (23) | –368* | 660* | 1044 | — |
| 11 | Eyjabakkajökull (24) | –867* | 813* | 734 | — |
| Svalbard | | | | | |
| 17 | Midre Lovénbreen (48) | –352 | 303 | –463 | –991 |
| 16 | Austre Broggerbreen (49) | –464 | 333 | –567 | –1244 |
| 15 | Kongsvegen (29) | –48* | 367* | –163 | — |
| 18 | Hansbreen (27) | –431* | 512* | –436 | — |
| Northern Scandinavia | | | | | |
| 20 | Engabreen (46) | –8 | 948 | 610 | –260 |
| 21 | Langfjordjøkelen (25) | –927* | 781* | –797 | –1664 |
| 22 | Marmaglaciaren (23) | –430* | 525* | — | — |
| 23 | Rabots Glacier (31) | –394* | 560* | — | — |
| 24 | Riukojietna (26) | –592* | 805* | — | — |
| 25 | Storglaciaren (69) | –75 | 678 | — | — |
| 26 | Tarfalaglaciaren (18) | –211* | 1101* | — | — |
| 27 | Rundvassbreen (8) | — | — | –20 | –488 |

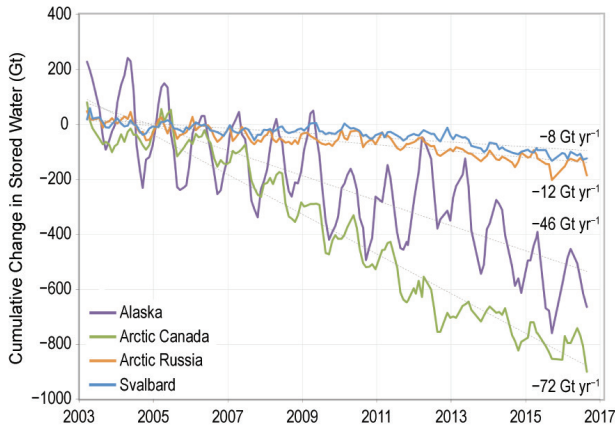


FIG. 5.16. Cumulative changes in regional total stored water for 2003–16 (Gt), derived using GRACE satellite gravimetry. Estimated uncertainty in regional mass changes is 8 Gt yr⁻¹ for the Gulf of Alaska, the Canadian Arctic, and the Russian Arctic, and 4 Gt yr⁻¹ for Svalbard. These errors include the formal error of the least squares fit and the uncertainties in the corrections for glacial isostatic adjustment, Little Ice Age, and terrestrial hydrology.

of regional total stored water estimates (Fig. 5.16), derived using GRACE satellite gravimetry available since 2003. Annual storage changes are a proxy for changes in the regional annual glacier mass balance (ΔM) for the heavily glacierized regions of the Arctic. Measurements of ΔM in 2015/16 for all the glaciers and ice caps in Alaska, Svalbard, and the Russian Arctic are inconclusive as the GRACE time series is currently only available through August 2016, and melt in these regions typically continues into September.

g. Terrestrial snow cover—C. Derksen, R. Brown, L. Mudryk, and K. Luojus

Snow cover is a defining characteristic of the Arctic land surface for up to 9 months each year, evolving

from complete snow cover in the winter to a near total loss by the summer. Highly reflective snow cover acts to cool the climate system, effectively insulates the underlying soil, and stores and redistributes water in solid form through the accumulation season before spring melt. Snow on land in spring has undergone significant reductions in areal extent during the satellite era (starting in 1967), which impacts the surface energy budget, ground thermal regime (with associated effects on geochemical cycles), and hydrological processes. The 2015/16 snow cover season (September 2015–June 2016) is reported here.

Snow cover extent (SCE) anomalies (relative to the 1981–2010 reference period) for land areas north of 60°N during spring (April, May, June) 2016 were computed separately for the North American and Eurasian sectors of the Arctic from the NOAA snow chart climate data record, which extends from 1967 to present (Estilow et al. 2015; <http://climate.rutgers.edu/snowcover>; Fig. 5.17). SCE anomalies over the North American sector of the Arctic were strongly negative in all three months: new record low anomalies were set for April and May, with the third lowest values in the NOAA dataset observed in June. Eurasian SCE anomalies were also negative in all three spring months, reaching the third lowest in the NOAA time series in June.

Although May Arctic SCE fell below 11 million km² only three times between 1967 and 2009, it has been below this level every year since 2009. Until 2008, June snow cover was below 4 million km² only once since 1967 (1990), yet it has been below this value every year since. (For reference, the average May and June SCE is 11.7 million km² and 5.3 million km², respectively, for the 1981–2010 base period.) The rate of change in May SCE in the NOAA snow chart data record is now -5.0% decade⁻¹, which is statistically

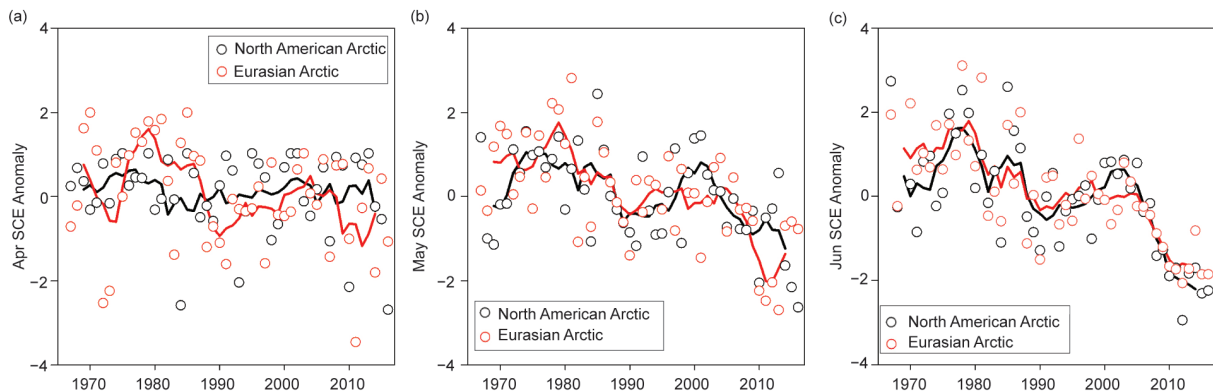


FIG. 5.17. Monthly snow cover extent (SCE) anomalies (1981–2010 base period) for Arctic land areas for (a) Apr, (b) May, and (c) Jun, from 1967 to 2016. Each observation is differenced from the average and divided by the standard deviation and thus unitless. Solid black and red lines depict 5-yr running averages for North America and Eurasia, respectively. (Source: NOAA snow cover extent CDR.)